# Antibody Array Analysis with Label-based Detection and Resolution of Protein Size*[S]

**Weiwei Wu‡, Heidi Slåstad‡§, Daniel de la Rosa Carrillo‡¶, Tom Frey‖, Geir Tjønnfjord§, Eva Boretti‡, Hans-Christian Aasheim**, Vaclav Horejsi‡‡, and Fridtjof Lund-Johansen‡§ §§**

**Elements from DNA microarray analysis, such as sample labeling and micro-spotting of capture reagents, have been successfully adapted to multiplex measurements of soluble cytokines. Application in cell biology is hampered by the lack of mono-specific antibodies and the fact that many proteins occur in complexes. Here, we incorporated a principle from Western blotting and resolved protein size as an additional parameter. Proteins from different cellular compartments were labeled and separated by size exclusion chromatography into 20 fractions. All were analyzed with replicate antibody arrays. The elution profiles of all antibody targets were compiled to color maps that resemble Western blots with bands of antibody reactivity across the size separation range (670–10 kDa). A new solid phase designed for processing in microwell plates was developed to handle the large number of samples. Antibodies were bound to protein G-coupled microspheres surface-labeled with 300 combinations of four fluorescent dyes. Fluorescence from particle color codes and the protein label were measured by high-speed flow cytometry. Cytoplasmic protein kinases were detected as bands near predictable elution points. For proteins with atypical elution characteristics or multiple contexts, two or more antibodies were used as internal references of specificity. Membrane proteins eluted near the void volume, and additional bands corresponding to intracellular forms were detected for several targets. Elution profiles of cyclin-dependent kinases (cdks), cyclins, and cyclin-dependent kinase inhibitors, were compatible with their occurrence in complexes that vary with the cell cycle phase and subcellular localization. A two-dimensional platform circumvents the need for mono-specific capture antibodies and extends the utility of antibody array analysis to studies of protein complexes.** ***Molecular & Cellular Proteomics 8:245–257, 2009.***

From the Rikshospitalet Medical Center and the University of Oslo, ‡Department of Immunology, §Department of Medicine, Section for Hematology, and ¶Department of Dermatology, 0027 Oslo, Norway, ‖BD Biosciences, San Jose, California 95131, Department of Medical Genetics, **Ullevaal University Hospital, 0407 Oslo, Norway, and ‡‡Academy of Sciences of the Czech Republic, Institute of Molecular Genetics, Videnska 1083, CA-142 20, Prague 4Krc, Czech Republic

Received, April 18, 2008, and in revised form, August 11, 2008

Published, September 16, 2008, MCP Papers in Press, DOI 10.1074/mcp.M800171-MCP200

Cellular proteins interact with agonistic and antagonistic regulators, and their functions depend on post-translational modifications and sub-cellular localization. Although it is rational to measure multiple components simultaneously, large scale protein analysis remains a challenge. Mass spectrometry can be used to detect a thousand proteins in a sample and provides unmatched resolution of molecular detail (1–3). The protocols are, however, too laborious and time-consuming to be used for screening purposes. During the past years, efforts have been made to develop platforms for proteins that are analogous to DNA microarrays (4–7). Assays based on multiplexed capture antibodies and matched detection reagents are available from several sources. The sandwich format provides dual specificity, but available assays are mainly limited to covering cytokines and a few selected signaling proteins. Moreover, signal-to-noise ratios decline when the number of detection reagents exceeds 20–40 (4–7). High throughput analysis of signaling proteins is possible with the reverse protein arrays described by Petricoin and colleagues (8) In these assays, the samples rather than the affinity reagents are multiplexed, and each array is labeled with a single or two antibodies.

The platform that currently allows detection of the highest number of proteins in a single sample is based on the use of protein labels for detection. All the proteins in the sample are reacted with haptens or fluorescent dyes, and the total amount of protein associated with each capture reagent is measured (9, 10). Sample labeling is adopted from DNA microarray technology and could in principle allow proteome-wide analysis. For cytokine measurement, the specificity and sensitivity is comparable with that of sandwich assays (11). Extending the principle to cellular proteins is, however, complicated by the lack of mono-specific capture reagents. The high content of protein complexes in cell lysates complicates analysis further (6, 12).

In Western blotting, antibody reactivity is resolved against protein size, to detect specific binding and cross-reactivity as discrete bands. Measurement with antibody arrays and label-based detection is comparable with Western blotting where the lanes have been compressed into a single band. The fact that non-specific bands in Western blots are frequent and sample-dependent is a strong argument against the current analysis platform (6). On the other hand, the principle of

resolving antibody reactivity against protein size could be adapted to array-based analysis. Here, we fractionated proteins by size exclusion chromatography and analyzed a series of fractions with replicate arrays to resolve protein size as a second parameter. Native separation yields liquid fractions of proteins in their functional context. A given protein may elute in non-overlapping fractions depending on its occurrence as a monomer or part of a complex. To compensate for the unpredictable elution profiles, we produced arrays containing two or more antibodies to each target as internal references of specificity.

Bead suspension arrays can be processed in microwell plates and are therefore well suited for analyzing a large number of sample fractions. A drawback is limited multiplexing capacity (5). The most sophisticated platform resolves 100 populations with different emissions of two fluorescent dyes and requires a dedicated instrument (13). To extend multiplexing, we examined whether polymer particles could be colored by surface labeling. A wide range of available dyes could potentially be used to generate complex color codes and allow the use of standard flow cytometers. We also determined whether Fc-binding affinity reagents could be used to anchor antibodies to bead suspension arrays. Affinity-based coupling would be compatible with small amounts of crude antibody preparations but could potentially lead to crossover of antibodies between the particles.

## MATERIALS AND METHODS

*Cells, Chemicals, and Antibodies*—Human leukocytes were obtained from buffy coats and CD4+ cells were purified and activated using Dynabeads with CD4 and CD3/CD28, respectively, as recommended by the manufacturer. The cells K562 (chronic myeloid leukemia), Jurkat (proT-ALL), Nalm-6 (B-ALL), THP1 (AML-M4), NB4 (AML-M3), and HEK293T (embryonic kidney) were cultured in RPMI with 20 mM HEPES and 5% fetal bovine serum. Unless otherwise stated, chemicals were from Sigma-Aldrich and fluorescent dyes from Invitrogen. Gamma globulins from mouse and goat and streptavidin-phycoerythrin (PE)[1] were from Jackson ImmunoResearch Laboratories.

*Production of Antibody Arrays*—Amine-functionalized polymethylmethacrylate-based particles with a diameter of 6 $\mu$m were from Bangs Laboratories. The particles were slightly hydrophobic, and unless otherwise stated, all buffers were supplemented with 1% Tween 20 and 1 mM EDTA to prevent aggregation and reduce nonspecific binding. Between all reaction steps, particles were washed twice by centrifugation at 1000 $\times$ *g* for 3 min, the supernatant discarded, the pellet vigorously resuspended on a whirlmixer and the particles suspended in the buffer used for the next reaction step. In the first step, particles (10% solids in PBS) were reacted with 3-(2-pyridyldithio) propionic acid *N*-hydroxysuccinimide ester (SPDP) (3 mg per gram of particles). The particles were rotated for 30 min at 22 °C. The pyridyl disulfide group was next reduced with 5 mM Tris (2-carboxyethyl)phosphine hydrochloride (TCEP) for 20 min at 37 °C and particles resuspended in 100 mM MES without detergent. Protein G (Fitzgerald Industries) was dissolved at 5 mg/ml in PBS, reacted with 100 $\mu$g/ml 4-(*N*-maleimidomethyl)cyclohexane-1-carboxylic acid 3-sulfo-*N*-hydroxysuccinimide ester (sulfo-SMCC, 30 min, 22 °C) and transferred to 100 mM MES pH 5 without detergent using G-50 fine (GE Healthcare) spin columns. Two milligrams of protein G-SMCC was added per gram of particles. After 30 min of rotation at 22 °C, particles were resuspended in 100 mM MES pH 6. Equal aliquots of particles at 1% solids were incubated with 3-fold serially diluted fluorescent maleimides for 30 min at 22 °C under constant rotation. Differently labeled particles were washed once and split in new aliquots, each of which was reacted with 3-fold serial dilutions of the next dye. The starting concentrations were 100 ng/ml for Alexa 488 and Alexa 647 and Pacific Blue and 500 ng/ml for Pacific Orange. Labeled particles were resuspended in PBS with 1% bovine casein, and 2 $\mu$g of antibody was added per mg particles. For binding of monoclonal mouse antibodies, particles were first coupled to subclass-specific goat-anti-mouse IgG Fc. Particles were rotated with antibody for at least 30 min at 22° C, washed three times in PBS, and resuspended in PBS with 50% trehalose and 40 mg/ml non-immune gamma globulins from goat and mouse to prevent crossover of specific antibodies between particles. Particles with different antibodies were mixed and stored frozen in aliquots at −70 °C. Control experiments showed that particle integrity or resolution was not affected by freezing (not shown). Approximately 5% of the particle populations were coupled to polyclonal non-immune immunoglobulins from mouse and goat and used as references for background.

*Cell Lysis and Protein Labeling*—Cells were suspended in 140 mM NaCl, 50 mM HEPES, pH 8, 10 mM $MgCl_2$, 1 mM TCEP, and 0.1% Tween 20 (4-fold the packed cell volume) and lysed by performing a freeze-thaw step on dry ice (14). The lysis buffer was supplemented with proteinase inhibitors (Sigma catalogue no. P8340) and phosphatase inhibitors (Sigma catalogue no. P5726), immediately before the use. Membranes and nuclei were pelleted by centrifugation at 2000 $\times$ *g* for 15 s. The supernatant was harvested as the hydrophilic fraction. The pellet was solubilized with 2% lauryl maltoside and sonicated for 10 s to extract membrane-associated and nuclear proteins. The two fractions were centrifuged at 10,000 $\times$ *g* for 10 min and the supernatants, typically containing 5–10 and 1–4 mg/ml of protein, respectively, were labeled with 0.5 mg/ml biotin-$PEO_4$-NHS (Pierce) at 22 °C for 20 min. This label was recently found in two studies to be optimal for detection of cytokines (10, 15). Free biotin was removed by passing the proteins over a G50F spin column equilibrated with 140 mM NaCl, 40 mM HEPES, pH 7.4, and 0.1% Tween 20. Selective biotinylation of cell surface proteins was performed by incubating viable cells on ice in PBS with 0.5 mg/ml biotin-$PEO_4$-NHS for 30 min.

*Size Exclusion Chromatography*—Biotinylated cellular proteins (240 $\mu$l, corresponding to protein from 60-$\mu$l packed cell volume or 3–8 $\times$ $10^7$ cells) were filtered through a 0.2-$\mu$m centrifuge filter (Millipore), loaded onto a Superdex 200, 10/300 column (GE Healthcare) and separated on an Äkta FPLC system (GE Healthcare) at 4–8 °C using a flow rate of 0.5 ml/min. The running buffer consisted of 140 mM NaCl, 50 mM Hepes (pH 7.4), and 0.1% Tween 20. Fractions of 0.5 ml were collected. The protein concentration of the fractions ranged from 20 to 500 $\mu$g/ml. The column was calibrated with a high molecular weight standard kit from GE Healthcare.

*Incubation of Labeled Proteins with Arrays*—Frozen aliquots of bead suspension arrays were thawed, pelleted, and resuspended in PBS with 1% casein and 40 $\mu$g/ml of mouse and goat gamma

[1] The abbreviations used are: PE, phycoerythrin; PBS, phosphate-buffered saline; Cdk, cyclin-dependent kinase; SPDP, 3-(2-pyridyldithio) propionic acid *N*-hydroxysuccinimide ester; TCEP, Tris(2-carboxyethyl)phosphine hydrochloride; MES, 4-morpholineethanesulfonic acid; SMCC, 4-(*N*-maleimidomethyl)cyclohexane-1-carboxylic acid 3-sulfo-*N*-hydroxysuccinimide ester; ex, excitation wavelength; BP, emission band pass filters; MNC, mononuclear cells; B2M, beta 2 microglobulin; INK, inhibitor of CDK4; *NHS*, *N*-hydroxy-succinimidyl; MHC, major histocompatibility complex; PHA, phytohemeagglutinin.

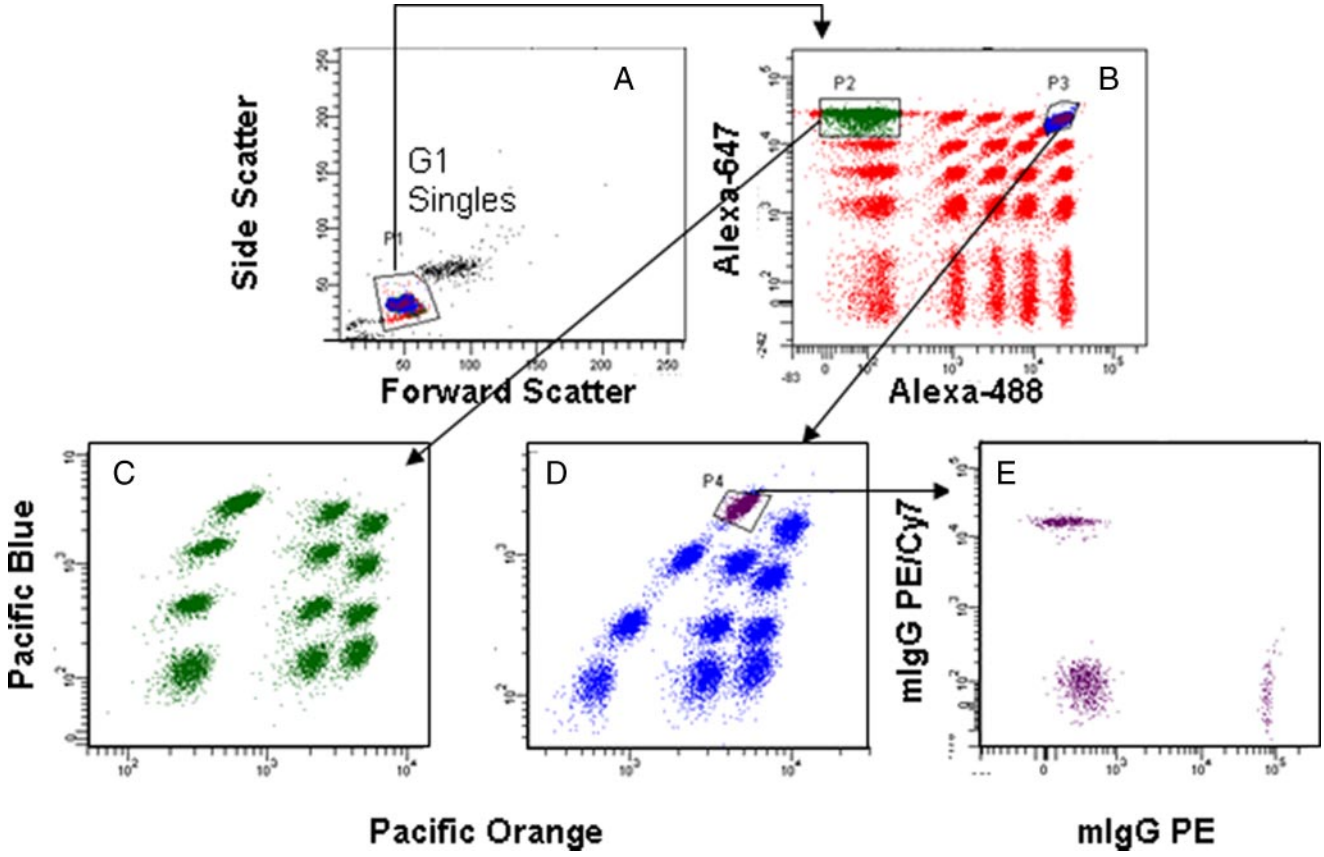


FIG. 1. **Particle arrays with four-dimensional color codes.** *A*, light scatter of particles region indicates gate for single particles. *B*, Alexa 488 and Alexa 647 fluroescence of single particles. *C* and *D*, Pacific Orange and Pacific Blue fluorescence of particles in indicated regions in *B*. *E*, antibodies show minimal crossover between particles. The particles in plots *A–E* are all measurements of a mixture of all the differently colored particles. Before flow cytometric measurement, the mixture was split in three aliquots, which were incubated separately with murine IgG-conjugated to PE, biotin and non-labeled mouse IgG, respectively. The particles were then washed, mixed in the presence of 40 $\mu$g/ml non-immune mouse and goat gamma globulins, and labeled with streptavidin-PECy7. *Plot E* shows that the three aliquots are detectable as populations with at least 2.5 logs of difference in fluorescence emission. The particles were analyzed at an acquisition speed of 3000 events per second.

globulins. Ten microliters of the suspension was added to wells of 96-well polypropylene PCR plates (Axygen). 100 $\mu$l of fractionated proteins was added, the volume adjusted to 200 $\mu$l with PBS, the wells capped, and plates rotated overnight at 4–8 °C in the dark. Particles were then pelleted by centrifugation, washed three times in PBS, and labeled with 10-$\mu$l streptavidin-PE (2 $\mu$g/ml in PBS with 1% bovine serum albumin). Labeled particles were washed twice in PBS and analyzed by flow cytometry.

*Immunoprecipitation and SDS-PAGE Analysis*—Immunoprecipitated proteins were visualized by a modification of the method published by Filatov *et al.* (16) Antibodies were bound to protein G-coupled polymer particles as described above and kept at 1% in PBS with 1% casein until use. Ten microliters of the bead suspension was added to 200-$\mu$l PBS containing 50 $\mu$g of Alexa 647-labeled proteins. The particles were rotated at 4 °C overnight and washed three times. Proteins were eluted by heating particles in PBS with 1% SDS to 95 °C for 5 min and separated on 8–16% SDS-PAGE gels. The gels were scanned with a Typhoon multi-mode fluorescence imager (GE Healthcare).

*Flow Cytometry and Data Analysis*—An LSRII flow cytometer was used to collect data (BD Biosciences). Excitation wavelength (ex) and emission band pass filters (BP): Pacific Blue and Pacific Orange, 405 nm ex; 450 BP and 530 BP, respectively; Alexa 488, PE 488 nm ex, 530 BP and 585 BP. Alexa 647 ex = 633 nm; 655 BP. Gates were set as shown in Fig. 1. Linearized values for median PE fluorescence for all particle populations were extracted by the FACSDiva software and exported to Excel spreadsheets. Data were formatted in Excel by matching the rows with a table for the antibodies and the file stored as tab-delimited text for analysis with the publicly available programs "Cluster" and "TreeView" from Michael Eisen's laboratory (17).

## RESULTS

*Multiplexing of Polymer Particles by Fluorescent Surface Labeling*—Polymer particles with surface thiols were first coupled to maleimide-derivatized protein G. Residual thiols were used to bind maleimide-derivatives of the four fluorescent dyes Alexa 488, Alexa 647, Pacific Blue, and Pacific Orange. The *upper right panel* in Fig. 1 shows particles that were labeled in sequence with five different concentrations of Alexa 488 and Alexa 647, respectively. Each of the 25 populations was split in 11–12 new aliquots that were labeled with different concentrations of Pacific Blue and Pacific Orange. Fluorescence from Pacific Orange and Alexa 488 were collected

with similar emission filters. The resolution of Pacific Orange was lower for particles with the highest levels of Alexa 488 because of fluorescence energy transfer from Pacific Blue (Fig. 1, *plot D*). Yet, the total number of unique particle subsets obtained was close to 300. Multiplexing could further be extended by variation of particle size (not shown). The particles were well resolved when acquired at 2000–3000 events per second. For details on precision of particle identification see supplemental Fig. 1.

Antibodies were bound to differently colored particles via protein G. Because binding is non-covalent, we examined the extent of crossover. A mixture of all particle subsets was incubated with goat-anti-mouse IgG1. Three aliquots were incubated separately with mouse antibodies conjugated to PE, biotin, or non-conjugated IgG, respectively. The particles were pooled and labeled with PE-Cy7-conjugated streptavidin. The results in Fig. 1 show three well defined populations separated by 2.5 logs of fluorescence intensity. Thus, the extent of crossover of antibody between the particles was less than 1%.

*Antibodies to Leukocyte Membrane Proteins Cluster According to Reactivity Profiles*—As an initial test of assay performance particle arrays with antibodies to leukocyte membrane proteins were incubated with biotinylated whole lysates of blood mononuclear cells. The best reagents showed linearity of the signal over a 100-fold difference in total protein content and a signal-to-noise ratio of more than 100 at the optimal concentration of lysate. Positive signals were detected using as little as 4 ng of total cell lysate equivalent of a few thousand cells. All the antibodies in Fig. 2*A* showed signal above background when the experiment was started using $10^4$ mononuclear cells (MNC) ($n = 3$, not shown).

The specificity of antibodies to leukocyte membrane proteins was tested by comparing reactivity to samples known to be enriched or depleted for the antigens, respectively. Subcellular fractions enriched for hydrophilic or membrane-bound proteins, respectively, were obtained by sequential lysis of MNC in 0.1% Tween 20 and 2% lauryl maltoside as described under "Materials and Methods". Two different antibodies to each target were included when available. The majority of the antibodies selectively captured protein from the membrane-enriched fraction of leukocyte lysates (Fig. 2*B*). Antibodies that bound proteins from the non-hematopoietic cell line HEK293T were against broadly expressed markers such as CD29, CD71, CD147, CD222, and MHC class I (Fig. 2*B*, *right*). The assay identified the expected PHA-induced up-regulation of leukocyte activation markers including CD71, CD54 (ICAM-1), and MHC molecules. SDS-PAGE of fluorescently labeled proteins confirmed that that most of the antibodies captured a single dominant species or a well defined complex such as MHCI/beta 2 microglobulin; (B2M) (Fig. 2*C*).

Leukocyte membrane proteins eluted early from the size exclusion chromatography column (Fig. 2*B*). The reason is likely to be that integral membrane proteins are purified in association with residual lipids and detergent micelles (18). Interestingly, the elution profiles of individual proteins were still sufficiently characteristic to group antibodies to the same proteins by cluster analysis. The antibody listing in Fig. 2*B* was generated by a computer algorithm that lists antibodies with similar reactivity profiles next to each other. Antibodies that were used repetitively in two different arrays that were processed separately clustered as nearest neighbors (Fig. 2*B*). The average correlation of these parallel measurements was $>0.9$ demonstrating high reproducibility of the assay (Fig. 2*B* and not shown). Importantly, different antibodies to the same protein also clustered. These results show that overlap in reactivity patterns of two or more antibodies to the same target may resolve specificity for targets that fail to elute as predicted from size.

*Size Exclusion Chromatography Resolves Intracellular Forms of Leukocyte Membrane Proteins*—A simplistic interpretation of the results in Fig. 2 is that most of the reagents are mono-specific and that sample fractionation adds little value. However, because the data are linear, only the most dominant species are visualized. Log transformation revealed that many antibodies captured two or more targets (Fig. 3*A*). Antibodies to MHC class I bound two discrete targets in the hydrophilic (*i.e.* soluble in 0.1% Tween 20) fraction of the lysate (Fig. 3*A*, *top left*, *blue lines*). The two peaks in the elution profile overlapped exactly those of B2M. One eluted near the void volume similar to most membrane proteins in Fig. 2*B*. The next, however, corresponded well with the expected elution point of a monomeric MHCI·B2M complex (50 kDa). The antibody to B2M captured a third target that eluted as expected for monomeric B2M (14 kDa; Fig. 3*A*). B2M does not have any transmembrane domain and is hydrophilic. This is reflected in the results showing high content of B2M in the hydrophilic fraction.

The MHCI·B2M complexes that eluted according to size, are not likely to be associated with lipids and detergent micelles. We hypothesized that the target was intracellular. Surface proteins were selectively biotinylated by incubation of viable cells with membrane-impermeable biotin. In lysates of surface-labeled cells, the peak at 30–60 kDa was absent (Fig. 3*A*, *top right*). Thus, the protein is likely to be intracellular.

Results similar to those for MHC class I and B2M were observed with the CD14 antigen. This surface protein also occurs as an intracellular form that is secreted (19). A protein eluting as expected for monomeric CD14 (55 kDa) was observed in samples biotinylated after cell lysis, but was minimal in samples where cell surface proteins were selectively labeled (Fig. 3*A*). The hydrophilic fraction contained almost exclusively the 55-kDa peak.

Typical log-transformed elution profiles of cell surface proteins are shown for CD4 and CD18 in Fig. 3*A*. The transmembrane adaptor proteins LAT, SIT, and CD3$\zeta$ showed a similar profile, except that additional peaks were observed near the expected elution point for the monomers (18–30 kDa) (Fig. 3*A*). The antibody to LAT captured three distinct targets, one

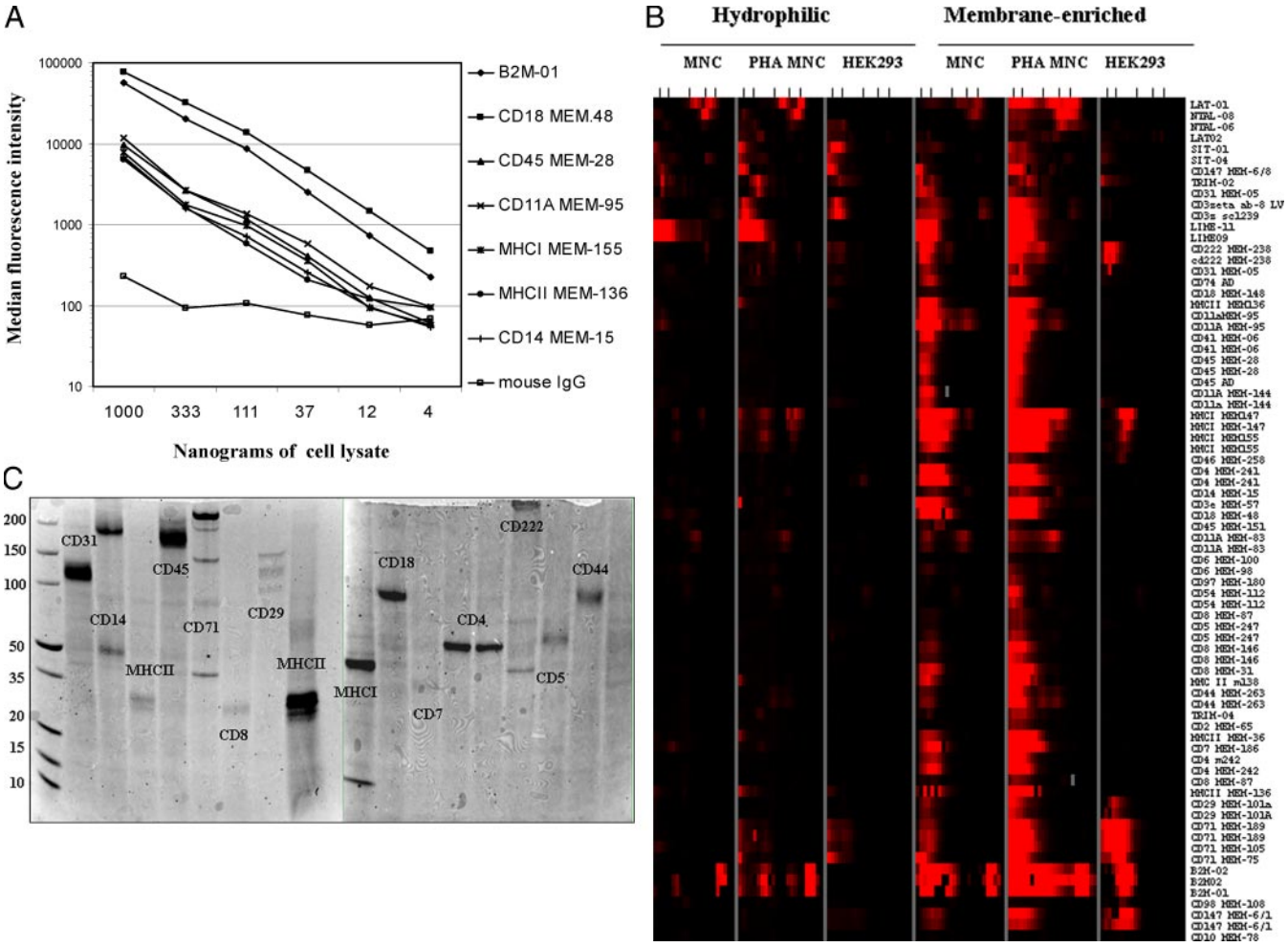


FIG. 2. **Antibody array analysis membrane proteins in leukocytes and HEK293T embryonic kidney cells.** *A*, blood MNC were lysed in PBS containing 1% lauryl maltoside. Proteins were biotinylated and indicated amount of total cell lysate incubated overnight with particle arrays in a total volume of 20 $\mu$l. Particles were washed and labeled with PE-conjugated streptavidin to detect captured protein and analyzed by flow cytometry (as described in the legend to Fig. 1). The data show median PE fluorescence intensity of particles with indicated antibody or non-immune mouse IgG. The data are from one experiment representative of three. *B*, freshly isolated blood MNC, PHA-blasts (*PHA-MNC*), and HEK293T cells were lysed sequentially in 0.1% Tween and lauryl maltoside. Biotinylated proteins from the hydrophilic (Tween-soluble) and membrane-enriched (lauryl maltoside-soluble) fractions were separated by size exclusion chromatography and 20 fractions analyzed with replicate antibody arrays. The listing of antibodies was generated by a clustering algorithm. When the same antibody is listed twice, it was used in two separate arrays; each incubated in a separate well of a microwell plate. Values are linear and median centered across the *x*- and *y*-axes. The *color map* shows the relative amount of protein (median PE fluorescence) captured by each antibody in the fractions. Measurements above the median are indicated by *red pixels*. The numbers on *top* of each set refer to migration points for protein standards (670, 440, 153, 75, and 43 kDa). *C*, lauryl maltoside-solubilized leukocyte proteins were labeled with Alexa 647-NHS and separated by size exclusion chromatography. The first five 0.5-ml fractions were pooled, and 100-$\mu$l samples incubated overnight with polymer particles coupled to indicated specificities (selected from the list in *B*). The particles were washed and boiled in SDS sample buffer and eluted proteins separated on 8–16% gradient gels. Gels were scanned with a Typhoon multi-mode imager. The results are representative of three experiments. All antibodies were from the Horejsi laboratory except those to CD3$\zeta$ (Labvision and Santa Cruz) and one anti-CD45 monoclonal antibody (Assay Designs).

early eluting species present exclusively in the membrane fraction and two more hydrophilic species eluting around 100 and 30 kDa, respectively (Fig. 3*A*, *bottom right*). The results are interesting because transmembrane adaptor proteins mainly have been studied in the context of detergent-resistant lipid rafts where they are often found in large complexes (20). The results on NTAL, a fourth member of the family, are surprising. This protein occurred predominantly in the late-eluting form. Two antibodies showed the same profile (see below), suggesting that NTAL may differ from the other members with regard to subcellular location and/or lipid association (Fig. 3*A*, *bottom left*).

Fig. 3*B* shows a color map where selected data from Fig. 2B were formatted to enhance visualization of reactivity in the hydrophilic and late eluting fractions where the content of membrane proteins was low. The elution profiles of MHCI/

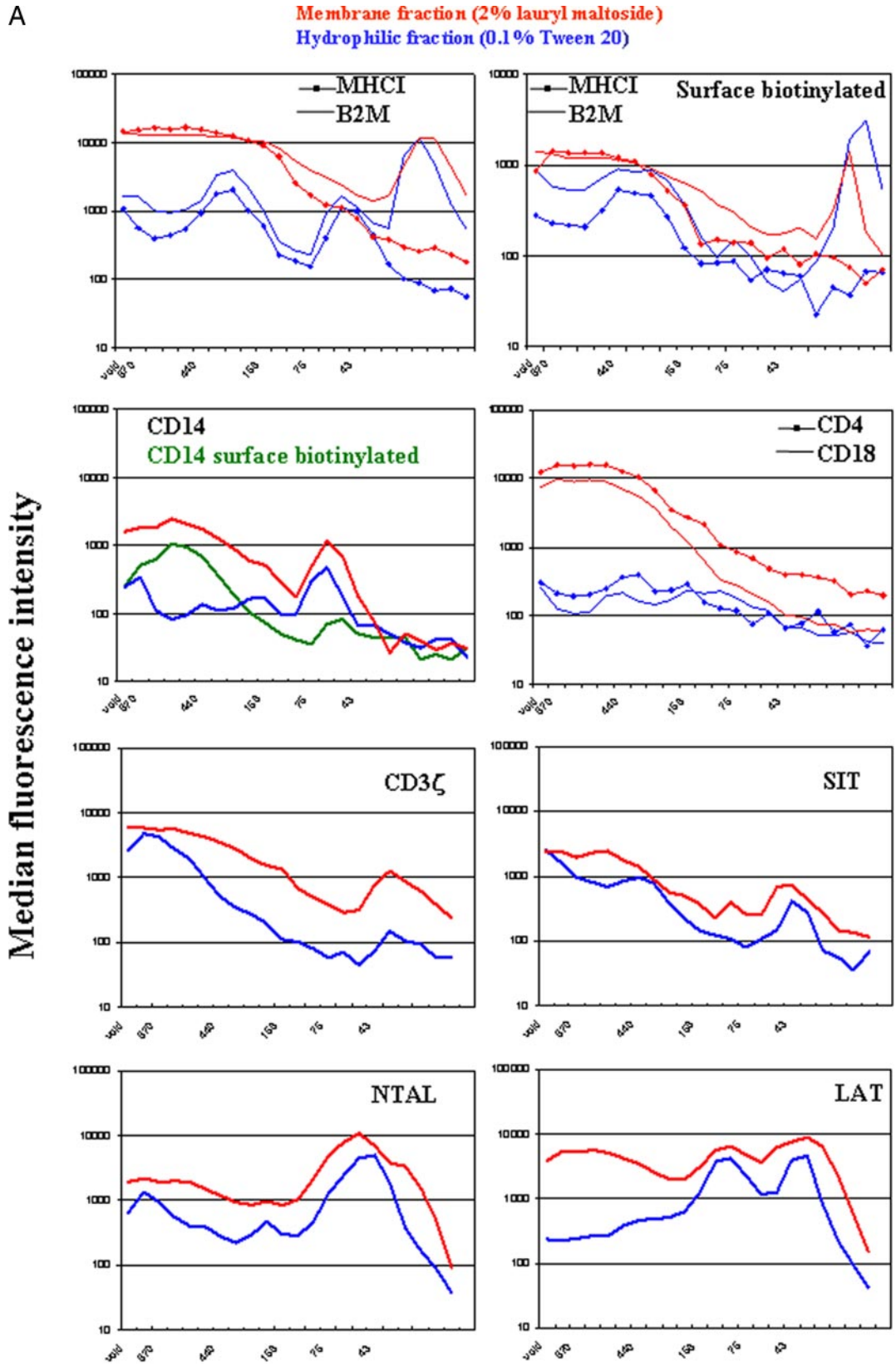


FIG. 3. **Discrimination of surface and intracellular forms of leukocyte membrane proteins.** *A*, the *line plots* show log transformed data from the same experiment as that described in legend to Fig. 2*B*. The results for MHC class I and CD14 were compared with samples where surface proteins were selectively biotinylated by incubation of viable cells with membrane impermeable biotin (MHC class I, *top right* and CD14,

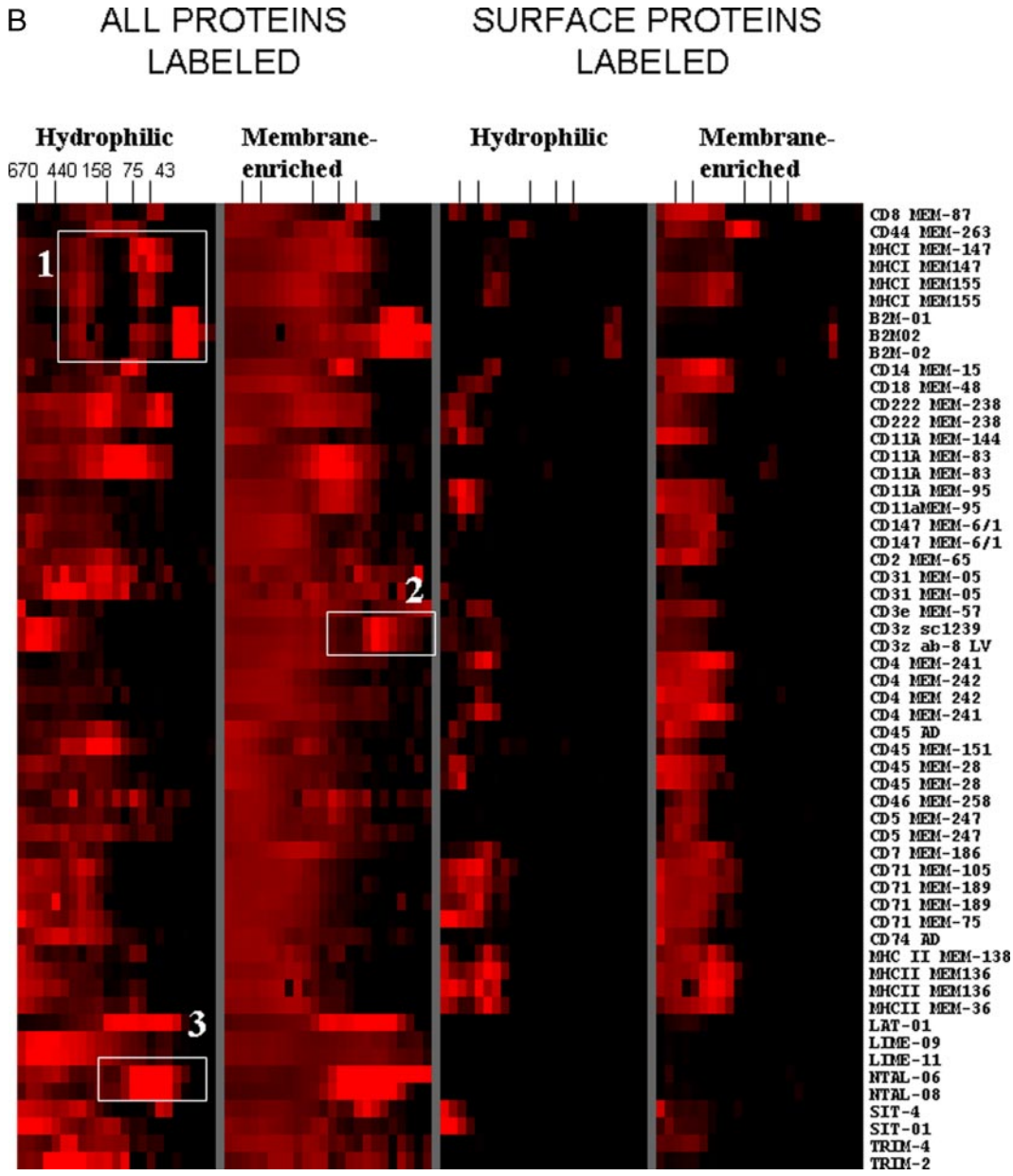


FIG. 3—*continued*

B2M (Fig. 3*B*, *box 1*), CD3ζ (*box 2*), and NTAL (*box 3*) were reproducible with two different antibodies to each target. Nearly all surface-biotinylated proteins eluted early (Fig. 3*B*, *right half*). In samples where proteins were labeled after cell lysis, capture of later-eluting forms was observed for several antibodies. These forms were best resolved in the hydrophilic fraction where they were more dominant. Collectively, the results support the view that fractionation of cell lysates by size exclusion chromatography provides information about the subcellular localization of membrane proteins. The com-

*green line*). The *red* and *blue lines* indicate proteins obtained from the membrane-enriched (lauryl maltoside-solubilized) and hydrophilic (0.1% Tween 20) fractions of the lysate, respectively. *B*, *color map* showing elution profiles of proteins labeled at the cell surface (*right half*) compared with proteins labeled after cell lysis. Values were log-transformed and median centered along the *x*-axis. Variations in signal intensity due to differences in protein concentration between fractions were adjusted for by normalizing values for the columns. This formatting adds weight to values in the late fractions where absolute concentration is lower. The listing of antibodies is manual. Antibodies that are listed twice were used in two different arrays that were handled separately. The lack of signal for transmembrane adaptor proteins in the surface-biotinylated sample is expected because the proteins lack lysines in their extracellular domains. The data are from a single experiment representative of three.

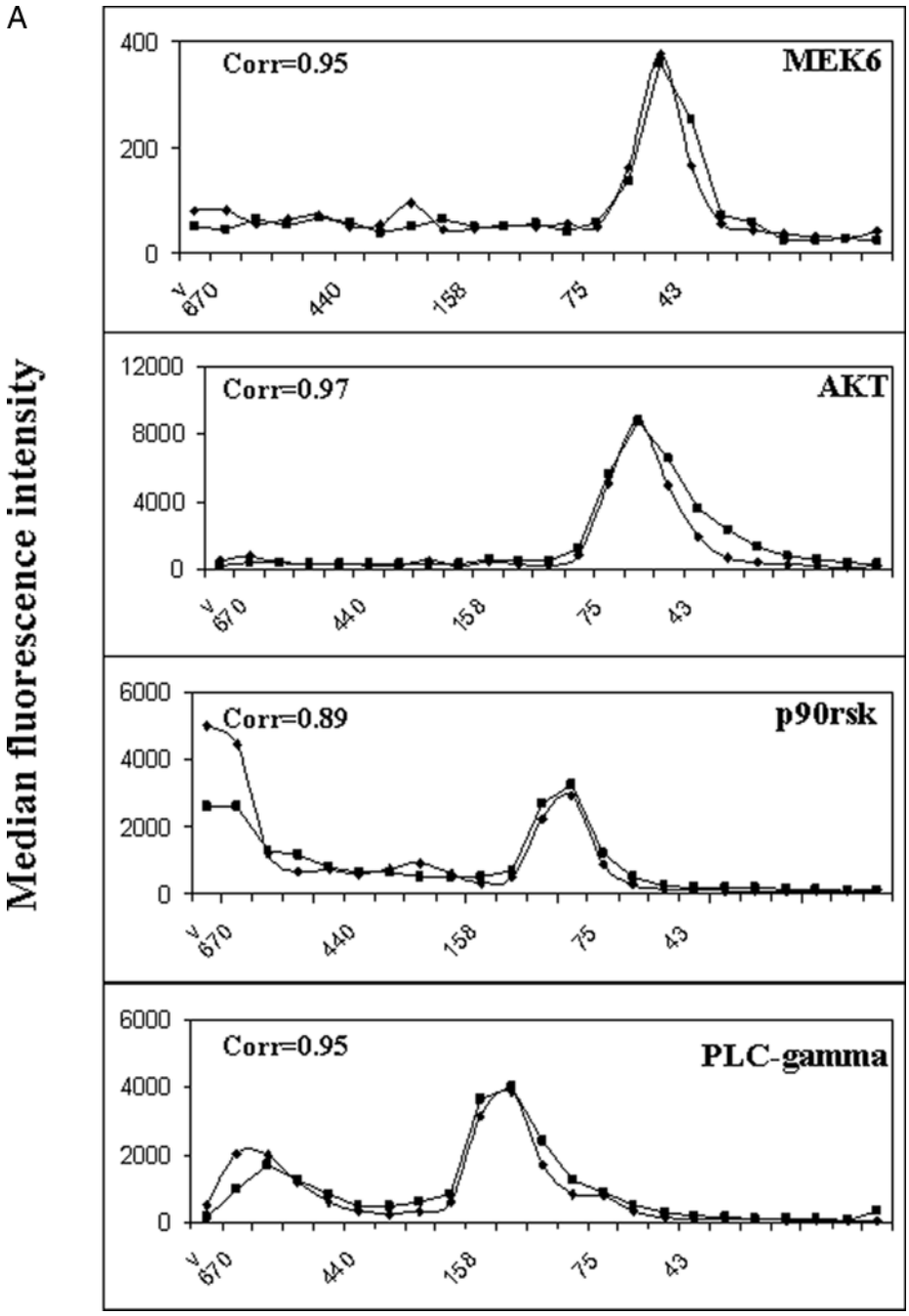


FIG. 4. **Antibody array analysis of intracellular proteins.** Hydrophilic (soluble in 0.1% Tween) proteins from *indicated cell lines* were biotinylated and fractionated by size exclusion chromatography. Twenty fractions from each cell line were analyzed with replicate antibody arrays as described in the legend to Fig. 2. *A*, elution profiles of targets for antibodies to MEK6 (Assay Designs), Akt (Upstate/Millipore), p90rsk (BD Biosciences), and PLC-gamma 1 (Upstate/Millipore) from HEK293T cells (kidney embryonic cells). *B*, color map of measurements from indicated cell line. The data were median centered along the *x*- and *y*-axes. Antibodies are listed according to the mass of the intended target (ascending order, top-down). The results are representative of three experiments.

plex elution profiles are also useful to determine antibody specificity.

*Reactivity Peaks of Antibodies to Intracellular Proteins Locate Near the Elution Points Predicted from Protein Size*—Migration of intracellular proteins was more related to protein size than that of membrane proteins. The peaks for phospholipase C gamma (140 kDa), p90rsk (82 kDa), Akt (55 kDa), and MEK6 (36 kDa), deviated slightly from the predicted elution points (Fig. 4*A*). However, this is an expected result, because additional factors such as molecular asymmetry influence migration of proteins through the resin. Two cell lysates were labeled and fractionated in parallel to determine reproducibility of the sample preparation process. The results correlated well (Fig. 4*A*), and when the void volume was omitted from analysis correlation coefficients were above 0.94 ($n = 3$). A significant amount of the protein captured by antibodies to p90rsk and PLC-gamma eluted as a separate wave near the void volume. This is likely to reflect capture of large complexes or antibody cross-reactivity. In an unfractionated lysate, measuring the captured biotinylated protein would overestimate the levels of the targets.

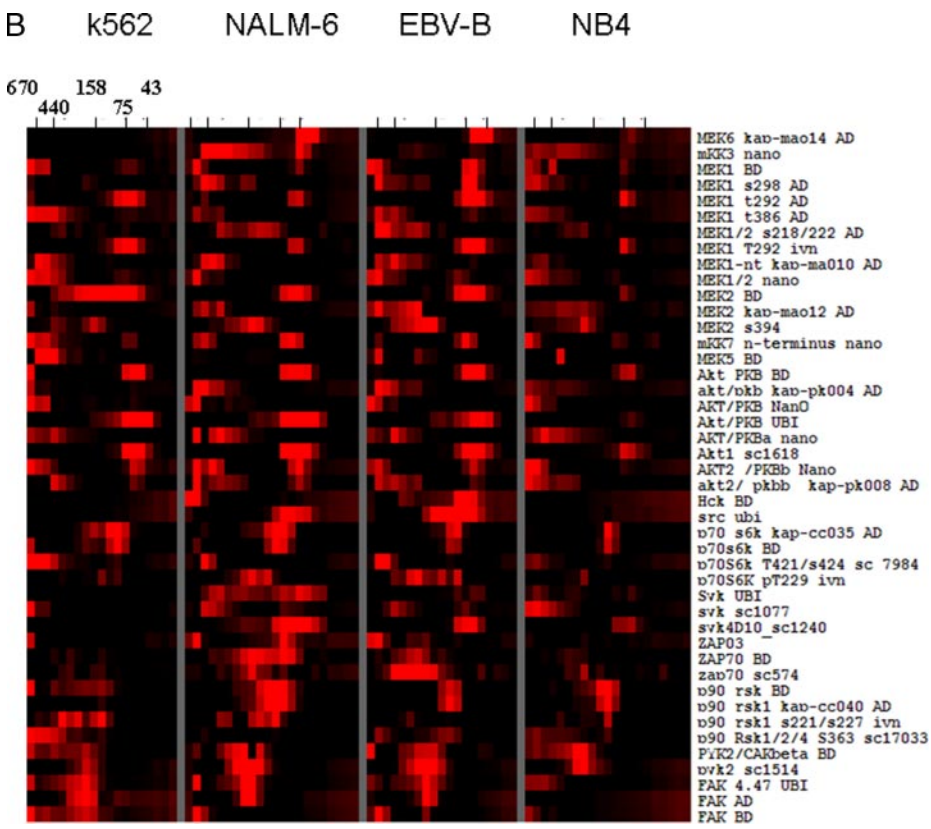


FIG. 4—*continued*

In Fig. 4*B*, the reactivity peaks of 45 antibodies in four cell lysates are visualized as bands in a color map. The antibodies are listed in ascending order according to the size of their intended targets (range: MEK6, 36 kDa; FAK, 120 kDa). Antibodies to the same or similar proteins frequently showed bands at the same position (Fig. 4*B*). The positions were similar in different cell lysates and corresponded well with the relative size of the intended targets. The distribution pattern of kinases among the cell lines provided further evidence for specificity. Ubiquitously expressed kinases including Akt, MEKs, p70S6K, and p90rsk were detected in all cell types, whereas ZAP-70, Syk, Hck, and Src were cell-type restricted (Fig. 4*B*). Several antibodies had additional, or exclusive, reactivity near the void volume (indicated as *red pixels* or near 670 Da), and the magnitude of this reactivity was unrelated to that near the predicted elution point of the intended targets. Bands near the void volume may therefore reflect non-specific capture of protein complexes. Collectively, the data in Fig. 4 show that relative protein size was reproducibly detected, and that the parameter is useful to discriminate specific binding and cross-reactivity.

*Alterations in the Cell Cycle Machinery following Exit of CD4+ T Cells from Quiescence*—The data in Fig. 3 show that the similarity in the elution profiles of two components of a protein complex (MHCI·B2M) was detected by antibody array analysis. This result demonstrates a potential of the technology in large scale identification of protein complexes. To further investigate this potential, we measured components of the cell cycle machinery. Several of these proteins occur in well defined complexes. For example, cdk inhibitors of the inhibitor of CDK4 (INK) family bind to cdk4 and cdk6 and inhibit binding of D cyclins (21) The elution profile of the cdk inhibitor p19/INK4d suggests the occurrence of the monomer at 20 kDa (Fig. 5*A*) and a larger species at 40–75 kDa. The overlaid elution profile of cdk6 revealed a peak overlapping almost exactly with the larger form of p19/INK4d (Fig. 5*A*). In quiescent cells, this appeared to be the dominant form of cdk6. In proliferating cells, there was a redistribution of cdk6 to larger forms. A peak around 200 kDa overlapped those of cyclin D3 and the cdk inhibitor p21 (Fig. 5*A*). The results are in accordance with previously published results showing that cdk6 interacts in mutually exclusive complexes with INK4 family members or D cyclins and p21 (14).

Cyclins A and B also co-eluted with their respective interaction partners, cdk2 and cdk1 (Fig. 5*A*). The antibodies to cdk1 and cyclin B1 showed additional reactivity near the void volume. These peaks were higher in quiescent cells and may represent cross-reactivity. The proliferation-dependent targets were readily detected as peaks distributed as expected for cyclin·cdk complex and monomeric cdk1, respectively (Fig. 5*A*).

Fig. 5*B* shows results obtained with a larger panel of antibodies to cell cycle regulatory proteins. Analysis of fractions enriched for chromatin-bound proteins is also in-

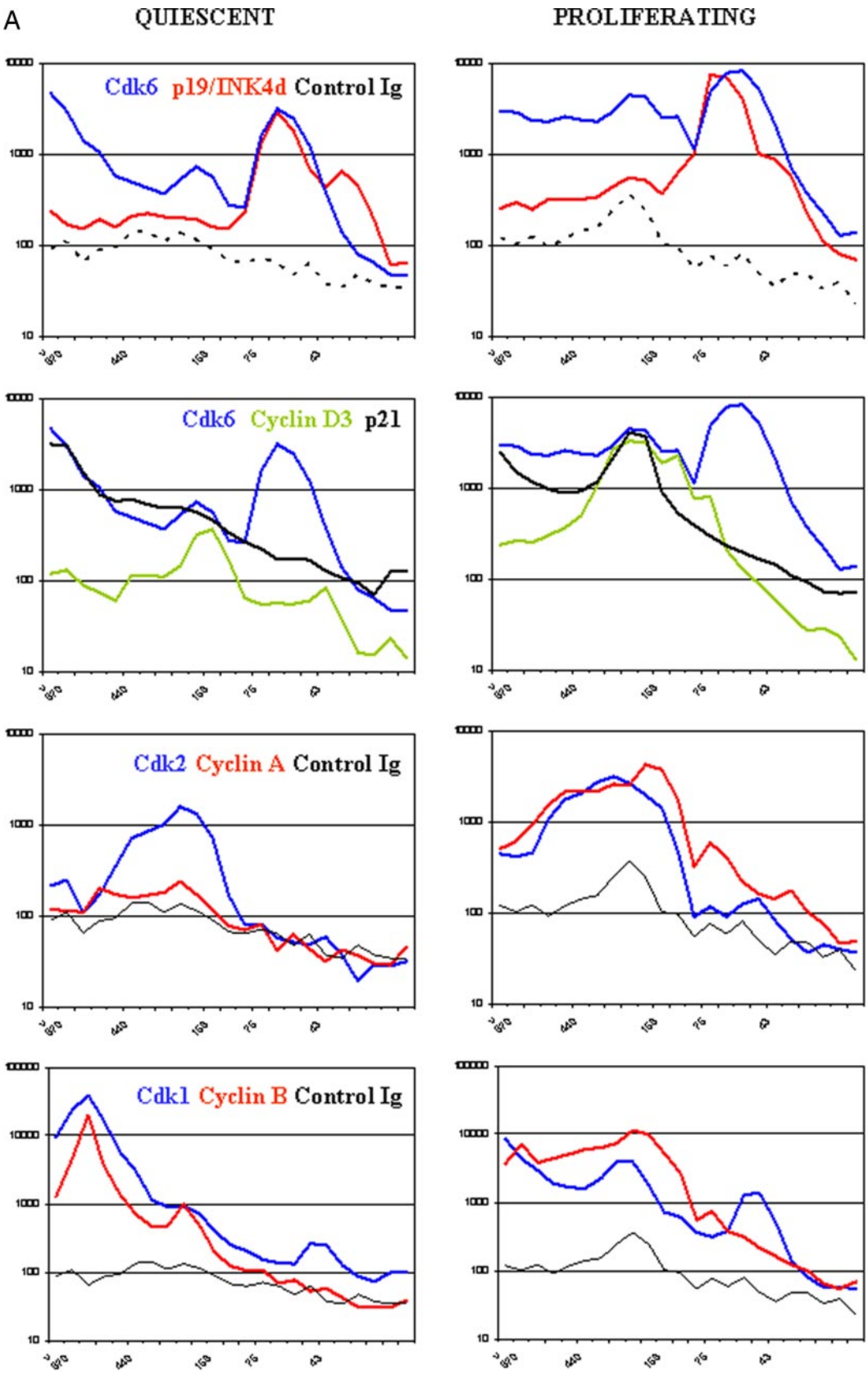

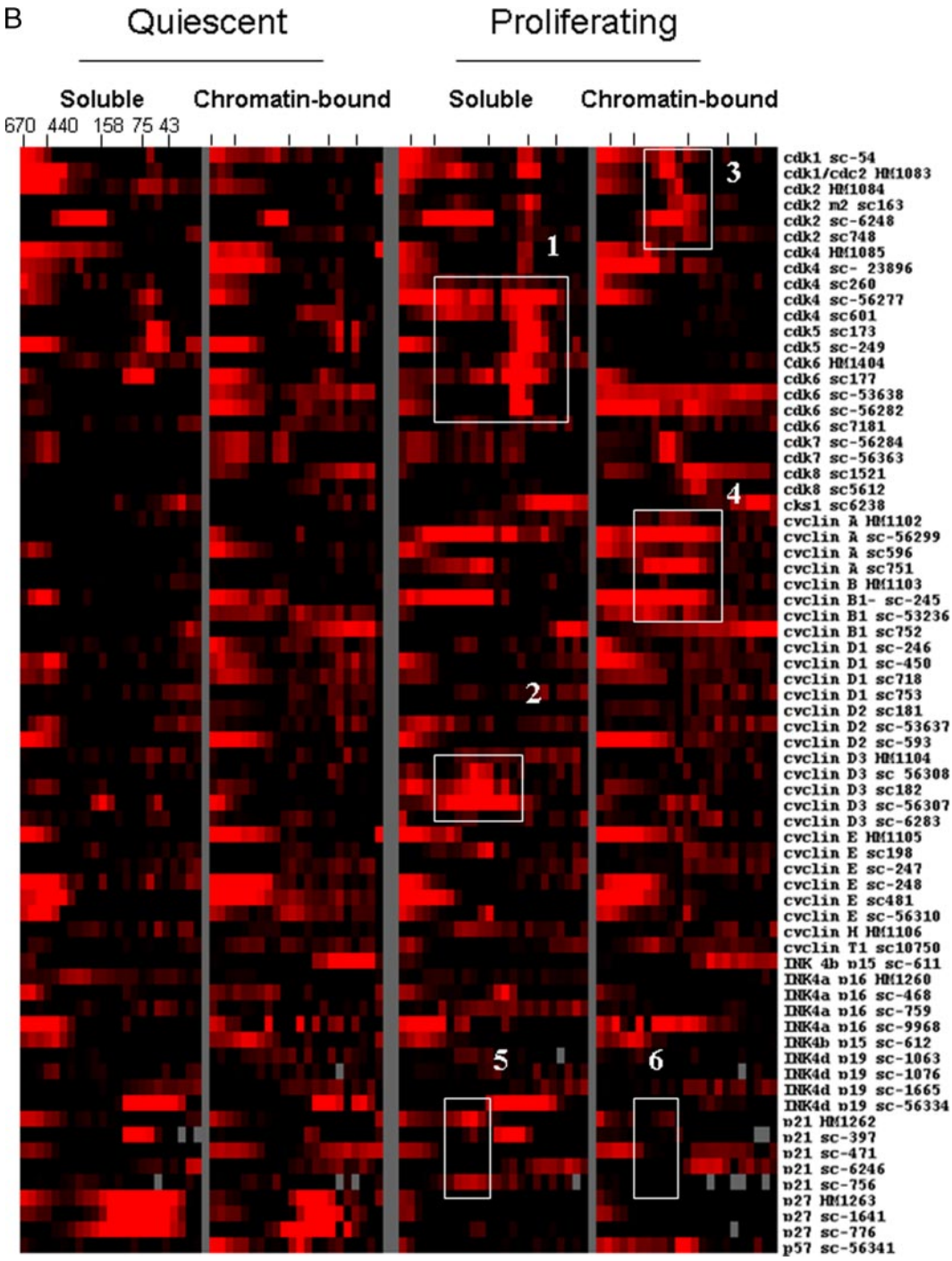


FIG. 5—*continued*

Fig. 5. **Antibody array analysis of the cell cycle machinery in CD4+ T cells.** CD4+ T cells were isolated from human blood and lysed immediately (*quiescent*) or after 48 h of stimulation with Dynabeads with anti-CD3 and -CD28 (*proliferating*). Lysates were labeled, fractionated, and analyzed by antibody arrays as described in the legend to Fig. 2. *A*, elution profiles of cdks, cyclins, and cdk inhibitors present in the Tween-soluble fraction of quiescent or proliferating cells. *B*, color map where the results from *A* are shown in the context of results obtained with additional antibodies and measurements of the fraction of the lysate enriched for membrane- and chromatin-bound proteins. Data were log-transformed and median-centered along the *x*- and *y*-axes. Variations in signal intensity due to differences in protein concentration between fractions were adjusted for by normalizing values for the columns. Antibody listing is manual. The figure is from a single experiment representative of four. The antibodies were selected on the basis of recommendation from the manufacturer for use in immunoprecipitation. Antibody sources: *sc*, Santa Cruz Biotechnology; *HM*, Hypromatrix.

cluded. Compared with the line plots in Fig. 5*A*, some detail was lost with the formatting required to visualize all antibody targets simultaneously. Yet, the similarity in the pattern of bands shows that the majority of results in Fig. 5*A* were reproducible with two or more different antibodies to the same protein. The same was true for measurement of cdk5, cdk7, and cdk8 (Fig. 5*B*). The expected down-regulation of the cdk inhibitor p27 upon exit from quiescence was detected with three different antibodies (Fig. 5*B*, *bottom*). Several antibodies showed bands near the void volume (Fig. 5*B*). In the case of cyclins, these bands are likely to represent cross-reactivity because the pattern was similar in quiescent and proliferating cells.

An interesting difference in the subcellular distribution of cdk·cyclin complexes was found in proliferating cells. Whereas D cyclins and cdk6 were restricted to the Tween-soluble fraction of the lysate (Fig. 5*B*, *boxes 1* and *2*), cdk2·cyclin A and cdk1·cyclin B were abundant in the fraction enriched for chromatin-bound proteins (Fig. 5*B*, *boxes 3* and *4*). The chromatin-bound fraction was enriched for the cdks forms that co-eluted with cyclins (Fig. 5*B*, *box 3*). The result is in accordance with previous studies showing that active form of cdk1·cyclin B and cdk2·cyclin A bind chromatin (22).

## DISCUSSION

Antibody array measurement with label-based detection was first published in 2001, and later studies have verified its utility for large scale measurement of cytokines (9). Yet, small scale assays with matched detection antibodies are by far dominating commercial products. Most likely, this reflects the difficulties associated with obtaining mono-specific antibodies and validating their performance. In an unfractionated sample, the proportion of the signal that derives from the intended target is not assessed. Because antibody cross-reactivity is frequent and sample-dependent, assumption of mono-specificity must be based on very extensive testing. Resolving protein size as a second parameter provides a solution to the specificity problem because different proteins binding to the same antibody are detected independently. The advantage is significant because very few antibodies have been shown to capture single target from a cell lysate. For example, MacBeath (6) reported that only 5% of commercial antibodies were useful for antibody array analysis of cell lysates.

In principle, antibody array analysis is a multiplexed form of immunoprecipitation. Provided that the intended target can be resolved from cross-reactivity, any antibody capable of immunoprecipitating its target should be useful. Still, we found that many reagents recommended by the manufacturer for use in immunoprecipitation failed to capture the labeled target (see Fig. 5*B*). It is possible that the labels used for detection interfere with the binding of some antibodies. The amount of amine-reactive label used here could theoretically modify 30% of the lysines. On the other hand, it is worth noting that immunoprecipitation is not usually tested very extensively by antibody manufacturers. When test results are available, captured proteins are typically detected by staining Western blots with antibodies that are specific for the intended target. Comparative results for different reagents are rarely shown. The need for better and more systematic quality control of antibodies is underscored by the experience from the Protein Atlas project led by Mathias Uhlen (13). Only 35% of the commercial reagents they tested performed satisfactory in standard applications such as immunohistochemistry and Western blotting (23). Antibody arrays may contribute significantly to better validation by allowing parallel testing of large numbers of antibodies under identical conditions.

New and elegant techniques for printing antibody arrays on slides allow far more multiplexing than the particles used here (10). Slides cannot be handled in microwell plates, but it is certainly possible to print replicate arrays on a single slide to simplify sample processing. The most important advantage of particles is wider access to multiplexing technology. Most likely, antibody arrays will have to be tailored for specific applications, and few laboratories are equipped to produce high quality planar arrays. The particle format is flexible and simple to scale up. The production and use of a 300-plex may be challenging for new users and requires access to a three-laser flow cytometer. However, even a 30-plex would represent a significant improvement compared with measuring proteins one at a time. This level of multiplexing should be achievable in most laboratories with access to a flow cytometer, either by use of colored particles on the market or by producing arrays as described here.

Ideally, antibody array analysis would be analogous to single-chip DNA microarray measurement. Sample fractionation is time-consuming, and algorithms for analyzing array results are designed for a single data point per target (17). It has been suggested that a new generation of affinity reagents dedicated for antibody array analysis will solve the specificity problem (7). Encouraging data have been published for antibodies to several inflammatory mediators in serum (11). It remains, however, to be determined if reagents with similar specificity can be obtained for most intracellular proteins or solve the problem of protein complexes. Several immunologists hold the opinion that polyspecificity is a fundamental feature of immune receptor recognition (24). At best, it will take many years to replace existing antibodies with a new generation of mono-specific reagents, and producing reagents that are specific for all their contexts is beyond current biotechnology. On short term, efforts to improve protein separation techniques and labeling conditions are likely to be more fruitful than attempting to produce truly mono-specific reagents.

Another argument in favor of fractionation is that important information may be obtained about subcellular localization and protein context. Cellular proteomes are modular, and measurement of complexes may be more important than

assessment of total protein levels (12). So far, interactomics has largely been based on protocols that involve transfection of yeast or cell lines with affinity-tagged proteins (25). An intriguing aspect of this study is the possibility of screening for protein complexes in primary cells and patient samples. The assay is currently limited to detecting a single component of each complex. Moreover, the chromatography resin only resolves complexes smaller than 600 kDa. This is clearly a limitation, because protein concentration was highest in the early fractions, and a large number of antibodies captured protein near the void volume. A rational next step is to expand the fractionation range and use affinity chromatography downstream. This may facilitate better identification of complexes and candidate interaction partners. The particle platform is compatible with extensive fractionation because samples are handled in microwell plates and each array analyzed within seconds. To characterize all the components of the identified complexes, it will be necessary to develop high throughput protocols for analysis of immunoprecipitates by mass spectrometry. Array-based screening of chromatography fractions followed by mass spectrometry of antibody-isolated targets may provide a powerful combination of throughput and resolution that is lacking in current interactomics. In conclusion, the present study shows that a two-dimensional analysis platform addresses many of the specificity problems associated with array-based proteomics and allows large scale detection of protein complexes.

* The costs of publication of this article were defrayed in part by the payment of page charges. This article must therefore be hereby marked "*advertisement*" in accordance with 18 U.S.C. Section 1734 solely to indicate this fact.

[S] The on-line version of this article (available at http://www.mcp.org) contains Supplemental Fig. S1.

§§ To whom correspondence should be addressed. E-mail: fridtjof.lund-johansen@medisin.uio.no.

REFERENCES

1. Wu, L., and Han, D. K. (2006) Overcoming the dynamic range problem in mass spectrometry-based shotgun proteomics. *Expert Rev. Proteomics* **3,** 611–619
2. Olsen, J. V., Blagoev, B., Gnad, F., Macek, B., Kumar, C., Mortensen, P., and Mann, M. (2006) Global, *in vivo*, and site-specific phosphorylation dynamics in signaling networks. *Cell* **127,** 635–648
3. Rush, J., Moritz, A., Lee, K. A., Guo, A., Goss, V. L., Spek, E. J., Zhang, H., Zha, X. M., Polakiewicz, R. D., and Comb, M. J. (2005) Immunoaffinity profiling of tyrosine phosphorylation in cancer cells. *Nat. Biotechnol.* **23,** 94–101
4. Haab, B. B. (2006) Applications of antibody array platforms. *Curr. Opin. Biotechnol.* **17,** 415–421
5. Kingsmore, S. F. (2006) Multiplexed protein measurement: technologies and applications of protein and antibody arrays. *Nat. Rev. Drug Discov.* **5,** 310–320
6. MacBeath, G. (2002) Protein microarrays and proteomics. *Nat. Genet.* **32, (suppl.)** 526–532
7. Wingren, C., and Borrebaeck, C. A. (2008) Antibody microarray analysis of directly labeled complex proteomes. *Curr. Opin. Biotechnol.* **19,** 55–61
8. VanMeter, A., Signore, M., Pierobon, M., Espina, V., Liotta, L. A., and Petricoin, E. F., 3rd (2007) Reverse-phase protein microarrays: application to biomarker discovery and translational medicine. *Expert Rev. Mol. Diagn.* **7,** 625–633
9. Haab, B. B., Dunham, M. J., and Brown, P. O. (2001) Protein microarrays for highly parallel detection and quantitation of specific proteins and antibodies in complex solutions. *Genome Biol.* **2,** RESEARCH0004
10. Ghatnekar-Nilsson, S., Dexlin, L., Wingren, C., Montelius, L., and Borrebaeck, C. A. (2007) Design of atto-vial based recombinant antibody arrays combined with a planar wave-guide detection system. *Proteomics* **7,** 540–547
11. Wingren, C., Ingvarsson, J., Dexlin, L., Szul, D., and Borrebaeck, C. A. (2007) Design of recombinant antibody microarrays for complex proteome analysis: choice of sample labeling-tag and solid support. *Proteomics* **7,** 3055–3065
12. Gavin, A. C., Aloy, P., Grandi, P., Krause, R., Boesche, M., Marzioch, M., Rau, C., Jensen, L. J., Bastuck, S., Dumpelfeld, B., Edelmann, A., Heurtier, M. A., Hoffman, V., Hoefert, C., Klein, K., Hudak, M., Michon, A. M., Schelder, M., Schirle, M., Remor, M., Rudi, T., Hooper, S., Bauer, A., Bouwmeester, T., Casari, G., Drewes, G., Neubauer, G., Rick, J. M., Kuster, B., Bork, P., Russell, R. B., and Superti-Furga, G. (2006) Proteome survey reveals modularity of the yeast cell machinery. *Nature* **440,** 631–636
13. Schwenk, J. M., Lindberg, J., Sundberg, M., Uhlen, M., and Nilsson, P. (2007) Determination of binding specificities in highly multiplexed bead-based assays for antibody proteomics. *Mol. Cell. Proteomics* **6,** 125–132
14. Parry, D., Mahony, D., Wills, K., and Lees, E. (1999) Cyclin D-CDK subunit arrangement is dependent on the availability of competing INK4 and p21 class inhibitors. *Mol. Cell. Biol.* **19,** 1775–1783
15. Kusnezow, W., Banzon, V., Schroder, C., Schaal, R., Hoheisel, J. D., Ruffer, S., Luft, P., Duschl, A., and Syagailo, Y. V. (2007) Antibody microarray-based profiling of complex specimens: systematic evaluation of labeling strategies. *Proteomics* **7,** 1786–1799
16. Filatov, A. V., Krotov, G. I., Zgoda, V. G., and Volkov, Y. (2007) Fluorescent immunoprecipitation analysis of cell surface proteins: a methodology compatible with mass-spectrometry. *J. Immunol. Methods* **319,** 21–33
17. Eisen, M. B., Spellman, P. T., Brown, P. O., and Botstein, D. (1998) Cluster analysis and display of genome-wide expression patterns. *Proc. Natl. Acad. Sci. U. S. A.* **95,** 14863–14868
18. Wiener, M. C. (2004) A pedestrian guide to membrane protein crystallization. *Methods* **34,** 364–372
19. Bazil, V., Baudys, M., Hilgert, I., Stefanova, I., Low, M. G., Zbrozek, J., and Horejsi, V. (1989) Structural relationship between the soluble and membrane-bound forms of human monocyte surface glycoprotein CD14. *Mol. Immunol.* **26,** 657–662
20. Horejsi, V. (2004) Transmembrane adaptor proteins in membrane microdomains: important regulators of immunoreceptor signaling. *Immunol. Lett.* **92,** 43–49
21. Jeffrey, P. D., Tong, L., and Pavletich, N. P. (2000) Structural basis of inhibition of CDK-cyclin complexes by INK4 inhibitors. *Genes Dev.* **14,** 3115–3125
22. Pines, J., and Hunter, T. (1991) Cyclin-dependent kinases: a new cell cycle motif? *Trends Cell Biol.* **1,** 117–121
23. Blow, N. (2007) Antibodies: the generation game. *Nature* **447,** 741–744
24. Wucherpfennig, K. W., Allen, P. M., Celada, F., Cohen, I. R., De Boer, R., Garcia, K. C., Goldstein, B., Greenspan, R., Hafler, D., Hodgkin, P., Huseby, E. S., Krakauer, D. C., Nemazee, D., Perelson, A. S., Pinilla, C., Strong, R. K., and Sercarz, E. E. (2007) Polyspecificity of T cell and B cell receptor recognition. *Semin. Immunol.* **19,** 216–224
25. Kiemer, L., and Cesareni, G. (2007) Comparative interactomics: comparing apples and pears? *Trends Biotechnol.* **25,** 448–454